MDPI

Article

A Heuristic-Driven Charging Strategy of Electric Vehicle for Grids with High EV Penetration

Bahman Ahmadi [1] and Elham Shirazi [2,*]

1   Department of Electrical Engineering, Mathematics and Computer Science, University of Twente, 7522 NB Enschede, The Netherlands; b.ahmadi@utwente.nl
2   Department of Engineering Technology, University of Twente, 7522 NB Enschede, The Netherlands
*   Correspondence: e.shirazi@utwente.nl

Abstract: The widespread adoption of electric vehicles (EVs) poses challenges associated with charging infrastructures and their impact on the electrical grid. To address these challenges, smart charging approaches have emerged as a key solution that optimizes charging processes and contributes to a smarter and more efficient grid. This paper presents an innovative multi-objective optimization framework for EV smart charging (EVSC) using the Dynamic Hunting Leadership (DHL) method. The framework aims to improve the voltage profile of the system in addition to eliminating voltage violations and energy not supplied (ENS) to EVs within the network. The proposed approach considers both residential EV chargers and parking stations, incorporating realistic EV charger behaviors based on constant current charging and addressing the problem as a mixed integer non-linear programming (MINLP) problem. The performance of the optimization method is evaluated on a distribution network with varying levels of EV penetration connected to the chargers in the grid. The results demonstrate the effectiveness of the DHL algorithm in minimizing conflicting objectives and improving the grid's voltage profile while considering operational constraints. This study provides a road map for EV aggregators and EV owners, guiding them on how to charge EVs based on preferences while minimizing adverse technical impacts on the grid.

Keywords: smart grid; electric vehicle; charging strategy; optimization algorithm; distribution network

1. Introduction

1.1. Background and Literature Review

The electrification of transportation through adopting electric vehicles (EVs) is gaining significant momentum worldwide as governments and industries strive to reduce greenhouse gas emissions and dependence on fossil fuels. EVs present a promising solution for achieving sustainable mobility. However, the widespread deployment of EVs poses several challenges, in particular, regarding charging infrastructure and the impact on the electrical grid. To address these challenges, smart charging approaches have emerged as solutions that optimize charging processes and contribute to the development of a robust and more efficient grid.

The global impact of gas emissions and fuel consumption is widely recognized, with the transportation sector being the largest contributor, accounting for over 20 percent of global energy consumption and greenhouse gas emissions [1]. However, electric vehicle adoption has surged globally to reduce pollution and lessen reliance on fossil fuels. Powered by batteries, ultracapacitors, and fuel cells, EVs offer a sustainable alternative to traditional fuel-powered vehicles, significantly minimizing harmful gas emissions. It is estimated that the number of EVs worldwide will reach approximately 130 million by 2030 [2].

The widespread adoption of EVs brings about significant challenges for the power sector. Unmanaged charging during peak hours can strain utility services, necessitating the expansion of production and transmission capacity. Current infrastructure may struggle to

handle increased demand, risking overloads and impacting transformer lifespans. Moreover, integrating EVs into grid stations can cause voltage fluctuations and increased power losses, introducing instability into power networks. This substantial integration also makes the power network more vulnerable to disruptions, leading to challenges in achieving a steady state. Concentrated power demand from numerous EVs in specific locations may result in elevated line losses and voltage violations, posing the risk of grid failures and interruptions in the electricity supply [3,4].

The rapid growth of EVs has spurred the need for more efficient and sustainable charging solutions. Conventional methods struggle to meet rising energy demands while ensuring grid stability. Smart charging optimizes energy resources, facilitates the integration of renewable sources, and promotes sustainable grid operation [5]. Smart charging enhances demand response by treating EVs as distributed energy resources within the smart grid. This integration allows real-time data and communication to optimize EV charging and discharging according to grid conditions and electricity demand [6,7]. This bi-directional energy flow optimizes renewable resource utilization, enhances grid stability, and increases the overall efficiency and reliability of the smart grid [8].

Smart charging approaches for EVs offer dual benefits at both the grid and individual user levels. Growing EV numbers and simultaneous peak-hour charging strain the grid, causing congestion. Smart charging strategies, such as time-of-use pricing and load-balancing algorithms, help spread the load by optimizing charging times throughout the day. This reduces grid stress during peak hours and minimizes the need for expensive infrastructure upgrades [9,10].

Furthermore, at the user level, smart charging provides personalized benefits. Intelligent algorithms analyze real-time data to determine the most cost-effective and convenient charging times for each EV owner, considering factors such as energy prices and user schedules. This customization enhances user satisfaction, maximizes renewable energy utilization, and reduces overall energy consumption [9,11]. By empowering EV owners with smart charging capabilities, these approaches promote widespread EV adoption and accelerate the transition to a sustainable transportation system.

Additionally, integrating EV charging with renewables enables coordinated energy use, boosting efficiency and sustainability. This supports broader goals of energy independence, reduced emissions, and decreased reliance on fossil fuels for transportation, promoting clean energy adoption [12]. The symbiotic relationship between EVs and the smart grid maximizes the potential of renewable energy while contributing to a greener future for generations to come [13].

Implementing smart charging for EVs allows grid operators and energy providers to explore new business models and revenue streams. By collecting detailed data on EV charging patterns and energy consumption, service providers can offer value-added services such as optimized charging plans, energy management solutions, and demand response programs. These services improve the customer experience and allow the monetization of data from smart charging systems. Moreover, integrating EVs with the smart grid enables vehicle-to-grid (V2G) technology, where EVs can provide ancillary services to the grid, such as frequency regulation and energy storage. This emerging market of smart charging and V2G capabilities holds the potential for economic growth, innovation, and collaboration in the energy sector [14].

The literature review explores current research on smart charging for electric vehicles. It covers topics such as charging optimization algorithms, demand response strategies, grid integration techniques, and the impact on grid stability. Studies highlight the importance of smart charging for EVs in both charging stations and residential areas.

Electric vehicle smart charging (EVSC) represents a strategic solution to effectively address the complexities associated with managing EV charging within the power grid, as highlighted in [15]. EVSC systems are designed to optimize EV charging processes, particularly during off-peak hours, to align with the technical constraints of the grid. It is noteworthy that, on average, EVs are parked in garages or charging station lots for

nearly 95% of the day, emphasizing the need for efficient charging management [16]. The coordinated charging of EVs within the EVSC framework ensures satisfaction among EV owners while carefully considering grid characteristics, such as the selection of an appropriate number of EVs and charging/discharging locations within specified time intervals [17].

The impact of EVSC on power systems has been extensively studied, highlighting both positive and negative influences, as mentioned in the previous section. Researchers have reviewed the barriers and opportunities associated with the economics and development of public charging infrastructures [18]. Additionally, charging solutions and optimization techniques have been thoroughly examined, considering aspects such as centralized and decentralized charging scheduling [19], data mining approaches (unsupervised and supervised) [20], load forecasting at different time horizons [21], and photovoltaic-assisted charging solutions [22]. Control methods, optimization objectives, and the centralized/decentralized nature of EV charging have also been explored, along with their potential negative effects on power system operations [23]. Various surveys have focused on specific topics such as available chargers [24], cybersecurity of onboard charging systems [25], dynamic pricing mechanisms [26], and the integration of EVs in frequency regulation and power quality improvement efforts [27].

Unregulated EV charging within a grid experiencing a high EV penetration rate can exert significant stress on utility services and subsequently lead to peak demand and overloading of the transformers [28]. The preexisting components and infrastructure within the energy sector may not have been initially engineered to withstand this additional load, thus increasing the risk of overloading and potentially compromising the lifespan of critical equipment such as transformers [29,30]. Notably, residential EV chargers, operating as DC electrical devices, can introduce power system harmonics, thereby elevating the levels of total harmonic distortion (THD) in the grid [31]. These formidable challenges underscore the imperative for meticulous planning and essential system upgrades to guarantee the dependable and efficient assimilation of EVs into the grid.

The implementation of EVSC systems necessitates the engagement of an EV aggregator or a governing body tasked with overseeing the charging procedure [32]. The pivotal role played by the EV aggregator in the efficient management of EV charging cannot be overstated [33]. EVSC systems are strategically designed to address the intricate challenges associated with EV charging, encompassing both technical and economic considerations within the grid, as well as accommodating the preferences of EV owners who may seek to charge their vehicles during peak load periods. The EV aggregators assume a central role in scheduling EV charging operations and collaborating with other aggregators to ensure minimal disruption to the grid's functionality. Through effective coordination of the EV, aggregators can ensure the satisfaction of EV owners while also meeting the grid's requirements and optimizing the overall charging process.

In recent research, it is notable that optimization modeling for the smart charging strategy in a smart grid has been employed as a valuable tool to enhance various aspects of EV-related processes. However, it is imperative to acknowledge that these optimization models often necessitate certain simplifications. These simplifications are introduced with the objective of rendering the problem formulations amenable to mathematical optimization approaches [34].

One common approach involves the linearization of problem formulations [35]. In this approach, researchers aim to simplify the mathematical complexity inherent in EV-related optimization challenges [36]. Linearization techniques enable the transformation of intricate nonlinear models for smart grids into linear approximations, facilitating the utilization of well-established mathematical optimization methods for problem resolution. One of the simplifications commonly used in the papers is assuming fixed power delivery of the chargers to the EVs [9]. The power/energy delivered to the EV is a function of the voltage at the charger node of the smart grid [37]. Moreover, in a real test system, following the optimization outcome for EVSC will lead to increasing the energy not supplied (ENS) [38]

for the feeders experiencing the under-voltages and also early charging the EVs for the nodes with over-voltage problems.

While modeling can aim for perfection in representing real-world scenarios, achieving high fidelity can often lead to computational challenges [39]. In cases of highly detailed and accurate models, mathematical optimization approaches may struggle to efficiently solve complex problems, especially for online and intra-day scheduling, resulting in slower computations, which is impractical. Furthermore, some approaches considering the complex modeling are not scalable and are only designed for specific test scenarios. To overcome these challenges, heuristic approaches are utilized to solve the complex models [40–42]. Although these heuristics hold promise in improving the accuracy of modeling in EVSC problems, their inability to guarantee optimal solutions underscores the need for novel algorithms capable of more precise exploration of the solution space.

1.2. Contribution

In this study, we present a multi-objective optimization framework that harnesses the power of the Dynamic Hunting Leadership (DHL) method [43]. Our innovative framework is engineered to tackle a broad spectrum of objectives associated with EVSC, encompassing goals that pertain to the grid's operational efficiency as well as user-centric preferences.

One of the primary objectives of our study is to optimize the ENS to EVs by more accurate modeling for charging behavior while reducing congestion, which is a crucial factor in enhancing the resilience and reliability of the power grid. By achieving this optimization, we effectively maintain the voltage profile within the grid, mitigating voltage-related issues that can affect both EVs and other electrical appliances connected to the network. Additionally, our framework is instrumental in identifying strategies to alleviate congestion within the grid, thereby optimizing the allocation of resources and ensuring a seamless charging experience for EV owners.

To rigorously evaluate the effectiveness of our proposed optimization method, we undertake a comprehensive assessment using a complex 769-node distribution network. This network is chosen for its realistic representation of real-world scenarios, as it encompasses both medium voltage (MV) grid components and low voltage (LV) feeders. We simulate various levels of EV penetration to assess the adaptability and robustness of our framework under different conditions.

To ensure a realistic representation of EV charging behaviors within our model, we consider a wide range of charging scenarios, including residential EV chargers and public parking stations. What sets our study apart from previous research is our meticulous consideration of the constant current behaviors demonstrated by these chargers. This inclusion transforms the optimization problem into a mixed-integer nonlinear programming (MINLP) challenge, allowing us to capture the intricacies of real-world EV charging dynamics more accurately.

Furthermore, our research contributes to the field by conducting a comprehensive comparative analysis. We benchmark the performance of our MINLP-based optimization approach against other well-established optimization algorithms. This comparative analysis provides insights into the strengths and weaknesses of various methods and highlights the superiority of our proposed framework in addressing the challenges posed by complex EVSC optimization tasks. The framework results presented in this study serve as an invaluable roadmap for both EV aggregators and individual EV owners. It offers guidance on how to make informed charging decisions that align with user preferences while simultaneously minimizing any adverse technical impacts on the grid. Our research not only advances the field of EVSC but also contributes to the development of sustainable and grid-friendly solutions for the growing electric mobility landscape.

The following summarizes the major contributions of this study:

1.　　Multi-Objective Optimization Framework: This study introduces a multi-objective optimization framework that leverages the DHL method. This innovative framework

effectively addresses a wide range of objectives related to EVSC, encompassing both grid-centric and user-centric goals.

2. Enhanced Grid Resilience: One of the primary contributions of the research is the optimization of ENS to EVs. By accurately modeling charging behavior and reducing congestion, the framework enhances the resilience and reliability of the power grid. This optimization ensures a stable voltage profile, mitigating voltage-related issues that could affect both EVs and other connected electrical appliances.

3. Congestion Mitigation Strategies: This study offers valuable insights into congestion mitigation within the grid. By optimizing the allocation of resources, the framework identifies strategies to alleviate congestion, leading to a more efficient use of grid resources and a seamless charging experience for EV owners.

4. Realistic EV Charging Behavior Modeling: Unlike previous research that relied on simplifications, this study incorporates the constant current behaviors exhibited by EV chargers. This inclusion transforms the EVSC optimization problem into a more realistic MINLP challenge, capturing the intricacies of real-world EV charging dynamics.

5. Comprehensive Comparative Analysis: The research conducts a comprehensive comparative analysis, benchmarking the performance of the MINLP-based optimization approach against other well-established optimization algorithms. This analysis provides valuable insights into the strengths and weaknesses of different methods and demonstrates the superiority of the proposed framework in addressing complex EVSC optimization tasks.

6. Guidance for EV Aggregators and Owners: The framework results presented in this study serve as a valuable roadmap for both EV aggregators and individual EV owners. It offers guidance on making informed charging decisions that align with user preferences while minimizing adverse technical impacts on the grid.

7. Utilization of the DHL Algorithm for EVSC: The research marks the inaugural implementation of the DHL algorithm in addressing the EVSC challenge. This innovative algorithm effectively balances conflicting objectives, such as voltage profile improvement and user satisfaction, contributing to the advancement of EVSC solutions.

This paper follows the following structure: The formulation of the proposed problem is addressed in Section 2. Section 3 delves into the implementation of the optimization algorithm and EVSC framework. The test systems are comprehensively described in Section 4, while the results are analyzed meticulously in Section 5. Finally, Section 6 provides a concise summary of the conclusions reached in this study.

2. Problem Formulation

The proposed multiple-dimensional objective functions encompass a range of technical and user-based goals specific to a grid. These objectives are treated individually and optimized using an optimization algorithm by combining the objective function into a single objective function. By considering multiple objectives simultaneously, this methodology aims to find a solution that offers a trade-off between the different objectives. This enables decision-makers to not only follow the scheduling based on the technical perspective of the grid but also based on user-based satisfactory options.

In general, the formulation of an optimization problem can be expressed as follows:

$$\underset{wrt\ \vec{x}}{\text{minimize}}\ F(\vec{x}) = \{f_1(\vec{x}), f_2(\vec{x}), ..., f_n(\vec{x})\} \tag{1}$$

$$\text{Subject to : } \begin{cases} lb_i \leq x_i \leq ub_i, i = 1, 2, ..., d \\ h_i(\vec{x}) = 0, i = 1, 2, ..., p \\ g_i(\vec{x}) \geq 0, i = 1, 2, ..., m \end{cases}$$

In the given problem, we have three functions denoted as $f_i(\vec{x})$, $h_i(\vec{x})$, and $g_i(\vec{x})$, representing the ith objective function, equality constraints, and inequality constraints to be minimized, respectively. *lb* and *ub* are the lower and upper boundaries for the control

variables. The variables n, q, and p represent the number of objective functions, inequality constraints, and equality constraints in the equation, respectively.

The optimization problem seeks to find the values of the decision variables that minimize the objective function while satisfying all the constraints. The specific form and complexity of the objective function and constraints depend on the problem at hand and the mathematical modeling approach used.

In the subsequent section, comprehensive formulations of the objectives and constraints are presented. A predefined discretization of the time horizon into discrete time intervals is assumed to facilitate the modeling process. This discretization allows us to effectively analyze and optimize the system over the given time period. Note that the control variable for the problem ($\vec{x}$) is the charging power of the EVs in the grid.

2.1. Objectives

The objective function for enhancing the voltage profile of the grid is formulated as the sum of the squared voltage magnitude differences between the buses and a reference set point. This summation is performed over a defined period, such as a day. To account for any deviations in bus voltage magnitudes, a penalty function is incorporated. Additionally, the objective function incorporates the ENS associated with EVs.

The term ENS for each EV user refers to the energy shortfall encountered when fully charging EV batteries caused by resource constraints or operational problems within the system. It is calculated as the total of uncharged energy across all EV batteries at the end of the charging period. The mathematical formulation for the objective function is as follows:

$$F = [\sum_{i=1}^{N_T} (\sum_{j=1}^{N_{BUS}} (V_{i,j} - V_{i,j,ref})^2 + k_1 \times PVV_{i,j})] + k_2 \times \sum_{k=1}^{N_{EV}} ENS_k \tag{2}$$

$$PVV_{i,j} = \begin{cases} 0, & \text{if } 0.95V_{i,j,ref} < V_{i,j} < 1.05V_{i,j,ref} \\ 1, & \text{if other} \end{cases} \tag{3}$$

In this equation, $V_{i,j}$ represents the voltage magnitude of the j-th bus calculated using a power flow method at the time i. N_T denotes the total duration of the optimization period, and N_{BUS} and N_{EV} represent the number of buses and EVs in the feeder. The term $V_{i,j,\text{ref}}$ corresponds to the reference voltage magnitude for the j-th bus.

The first part of the objective function accounts for the squared differences between the actual bus voltage magnitudes and their reference values. This term aims to minimize deviations from the desired voltage levels. Additionally, a penalty term ($PVV_{i,j}$) is included to penalize bus voltage magnitude violations. The penalty term is defined in Equation (3), where a value of 0 is assigned if the bus voltage magnitude falls within a range from 0.95 to 1.05 times the reference voltage magnitude, and a value of 1 is assigned otherwise.

The second part of the objective function incorporates the ENS of EVs. This term, weighted by the constant k_2, accounts for the impact of EV charging/discharging activities on the system. k_1 and k_2 are constant quantities that penalize the F_{VPI}. Note that the goal is to find an optimal solution in which the penalty parts for the solution are zero. It is important to note that voltage profile improvement not only enhances the voltage magnitudes at the buses but also contributes to reducing active power losses by achieving a better balance between bus voltage magnitudes.

2.2. Problem Constraints

The network's continuous operation is determined through an AC power flow computation, employing the approach introduced in [9]:

$$\sum_{ji}^{N_L} P_{ji,t} - \sum_{ij}^{N_L} \left(P_{ij,t} + I_{ij,t}^2 \mathcal{R}_{ij} \right) + P_{i,t}^S = P_{i,t}^D + P_{i,t}^{EV}, \quad \forall i \in N_N, t \in N_T \tag{4}$$

$$\sum_{ji}^{N_L} Q_{ji,t} - \sum_{ij}^{N_L} \left(Q_{ij,t} + I_{ij,t}^2 \mathcal{X}_{ij} \right) + Q_{i,t}^S = Q_{i,t}^D, \quad \forall i \in N_N, t \in N_T \tag{5}$$

$$V_{i,t}^2 - 2 \left(\mathcal{R}_{ij} P_{ji,t} + \mathcal{X}_{ij} Q_{ji,t} \right) - Z_{ij}^2 I_{ij,t}^2 - V_{j,t}^2 = 0, \quad \forall ij \in N_L, t \in N_T \tag{6}$$

$$V_j^2 I_{ij,t}^2 = P_{ij,t}^2 + Q_{ij,t}^2, \quad \forall ij \in N_L, t \in N_T \tag{7}$$

The equilibrium for the flow of active/reactive power at each bus of the system is shown by Equations (4) and (5). These equations are expressed in terms of various components, including the power transmitted through the circuit between nodes i and j ($P_{ij,t}$, $Q_{ij,t}$), the active and reactive power generated by the substation at node i ($P_{i,t}^S$, $Q_{i,t}^S$), the active and reactive power losses ($I_{ij,t}^2 \mathcal{R}_{ij}$, $I_{ij,t}^2 \mathcal{X}_{ij}$), and the combined demand from the base load and electric vehicles ($P_{i,t}^D$, $P_{i,t}^{EV}$). Note that the term R refers to the resistance of the lines in the network.

Equation (6) is used to calculate the voltage drop across the grid. In this equation, V_j represents the magnitude of the voltage at node j. The variable $\mathcal{X}_{ij}$ refers to the reactance, and Z_{ij} refers to the impedance of the ij^{th} circuit, respectively. Furthermore, the voltage at the slack bus is assumed to remain constant at the reference point ($V_{SE,t} = V_{ref,1}$). Equations (8) and (9) describe the operation of EVs connected to i-th bus of the system. These equations govern the power consumption of the EVs and energy balance during the charging process.

Equation (8) ensures that the balance of energy for each EV is maintained throughout the charging duration, effectively keeping the battery's energy within its capacity. This equation is formulated in relation to several key factors: the capacity of the batteries for the EVs connected to bus i, denoted as $\overline{E}^{EV}i$; the initial state of energy for each EV, denoted as $E^{ini}i$; and the charged energy over time, represented as $P^{EV}i, t\Delta t$, which is further multiplied by the charger efficiency ($0 \leq \varepsilon \leq 1$). To ensure compliance with the energy balance constraint and supply the necessary energy to the EV, a slack variable called ENSi is introduced.

Constraint (9) sets a maximum limit on the active power consumption of the electric vehicle (EV) that is linked to node i at time t. The parameter P^{ch} denotes the power rating of the EV charger, and $\zeta_{i,t}^{EV}$ is a binary parameter indicating whether there is an EV connected to node i during time t. This constraint guarantees that the power consumed by the EV remains within the charger's capacity.

$$\text{ENS}_i = \overline{E}_i^{EV} - E_i^{ini} - \varepsilon \sum_{t=1}^{N_T} P_{i,t}^{EV} \cdot \Delta_t, \quad \forall i \in N_N, \tag{8}$$

$$P_{i,t}^{EV} \leq \zeta_{i,t}^{EV} P^{ch}, \forall i \in N_N, t \in N_T \tag{9}$$

$$P_{i,t}^{EV} = I_{i,t}^{charger} \cdot V_{i,t}^{charger} \tag{10}$$

where $I_{i,t}^{charger}$ is an integer value within a range from 6 to 32 Amper per phase of chargers.

3. Implementation of Optimization Algorithm for EVSC Problem

3.1. Dynamic Hunting Leadership Optimization Algorithm

The DHL algorithm [43] was inspired by the cooperative teamwork of hunters seen in the hunting process. The algorithm was developed as an alternative method to mathematical optimization for searching optimal solutions in a problem space more efficiently. It employs a social hierarchy and hunting strategy to model the process. The algorithm involves coordination between leaders and search agents, working together to find potential solutions. Over the term of iteration for the iterative process, the number of leaders tracking

the best solutions is gradually reduced, enabling a shift from exploration to exploitation and a concentrated focus from the agents on the best target.

The DHL algorithm, originally developed as a general optimization algorithm, has found applications in addressing complex problems such as MINLP. Its unique approach leverages a social hierarchy and hunting strategy to model the optimization process effectively. Within the algorithm, there is a dynamic coordination between leaders and search agents, who collaborate to identify potential solutions. Remarkably, the DHL algorithm has demonstrated exceptional performance in addressing various challenges, including complex smart grid problems. Specifically, it has shown remarkable effectiveness in solving optimization problems related to voltage regulation in distribution grids, such as the optimal tap position problem [43]. Note that both EVSC and optimal tap position problems are considered MINLP. This application showcases the algorithm's adaptability and prowess in tackling real-world issues, highlighting its significance in the field of optimization and its potential to revolutionize problem-solving processes across various domains.

The optimization process using the DHL method is included in the following steps.

3.1.1. Initializition

To start the process, a set of potential solutions is generated randomly. The set is denoted as **X** and can be represented as follows:

$$\mathbf{X} = \vec{X}_m : m = 1, 2, ..., N_h \tag{11}$$

where $\vec{X}$ is a collection of control variables for N_h solutions.

Each solution $\vec{X}_m$ in **X** consists of D control variables and can be expressed as:

$$\vec{X}_m = X_{m,1}, ..., X_{m,D} \tag{12}$$

The values of the control variables $X_{m,n}$ for the nth component of each solution satisfy the following inequality:

$$LB_n \leq X_{m,n} \leq UB_n \tag{13}$$

Here, the lower and upper bounds for the nth component of the solutions are denoted by LB_n and UB_n, respectively.

Each solution is ranked using the objective function value, and a subset of N_l best solutions is selected to be the leaders for evaluating the hunters in the next step.

$$\mathbf{F}^* = \vec{F}_\mu : \mu = 1, 2, ..., N_l \tag{14}$$

where $\mathbf{F}^*$ is the best objective function value for N_l solutions $\mathbf{X}^*$.

3.1.2. Main Loop of the Evaluation

The primary purpose of the main loop within the DHL algorithm, as described in Ahmadi et al. [43], is to enhance the objective function value for each agent in the context of a maximization problem. This improvement is achieved by iteratively updating the agents, guided by a set of N_l leaders. Notably, the number of leaders involved in each iteration of the optimization process is dynamically adjusted based on a discriminative function. This dynamic adaptation aims to strike a balance between the exploration and exploitation phases of the search process, facilitating a comprehensive exploration of the solution space in the initial iterations while exploiting promising regions to achieve better optimization results in the final iterations.

From the optimization perspective, the main objective of the central loop is to enhance the objective function value for every agent involved in the optimization process. This enhancement aims to reduce the objective function's value (in the minimization problem). It is achieved by systematically updating the agent, leveraging the guidance provided by a select group of N_l leaders, and effectively balancing the exploration and exploitation phases of the search process.

The DHL algorithm strategically employs a gradual reduction in the number of leaders, which allows it to prioritize exploitation around a promising solution while also limiting excessive exploration of the solution space. During the exploration phase, the algorithm dedicates its efforts to searching the entirety of the solution space thoroughly. This comprehensive exploration is crucial for identifying promising candidates and avoiding the potential pitfalls of being trapped in locally optimal solutions. Conversely, the exploitation phase relies on refining the candidate solutions discovered during the exploration phase.

In the DHL algorithm, the evaluation of agents during each iteration of the main loop is impacted by the positions of a set of N_l leaders. The determination of N_l for each iteration follows a dynamic approach, allowing it to adapt based on the optimization progress. To facilitate this adaptability, a repository is established to maintain a historical record of the objective function values for the leaders, denoted as F^*. By referencing this repository, the algorithm can effectively update the value of N_l, ensuring a responsive and well-informed optimization process.

In the initial iteration, N_l equals the number of agents, denoted as N_h. This initialization allows for a balanced starting point, wherein all hunters possess leadership roles before the dynamic adjustments take effect.

The DHL algorithm reduces the number of leaders by assessing the objective value of the worst leader. The term "worst leader" denotes the leader in the set F^* with the highest objective function value (F). To achieve this, the current F value is compared against a predefined percentage of previous iterations.

Whenever the improvement in the objective function value, represented by F, falls below a specified threshold, it signifies inadequate progress. To address this, we adopt a systematic approach, eliminating the leader with the worst performance from the current set of leaders. This process is then iteratively applied to the remaining leaders until only one leader remains throughout the optimization process.

By iteratively eliminating underperforming leaders, this approach seeks to prioritize the retention of leaders that consistently demonstrate improved objective function values, thereby enhancing the overall optimization outcomes.

The process of eliminating underperforming leaders is shown as follows:

$$N_l = \begin{cases} N_l - 1, & if \ |F_{it} - F_{(it-(\beta \cdot \mathrm{Max}_{it}))}| < \epsilon \\ N_l, & if \ \ \mathrm{otherwise} \end{cases} \tag{15}$$

$$\beta = \frac{\varphi \cdot \mathrm{Max}_{it}}{100} \tag{16}$$

where φ denotes a predefined number between 1 and 100, and ϵ represents a small value performing as tolerance. F_{it} represents the objective value of the worst leader in the set.

Within each iteration of the hunting phase, leveraging the N_l leaders obtained from Equation (15), the positions of the remaining agents ($\vec{X}_m$) are subsequently updated using a set of equations. The following equations govern this updating process:

$$\vec{X}_{m,it+1} = \frac{\sum_{i=1}^{N_l}(\vec{X}_{l,it}^i - \rho \cdot |\vec{r}_2 \cdot \vec{X}_{l,it}^i - \vec{X}_{m,it}|)}{N_l} \tag{17}$$

$$\rho = 2 \cdot (1 - \frac{it}{\mathrm{Max}_{it}}) \cdot (2 \cdot \vec{r}_1 - 1) \tag{18}$$

Here, $\vec{X}_{l,it}^i$ indicates the position of the ith leader at the current iteration of the main loop. Similarly, $\vec{X}_{m,it}$ represents the position of the m_{th} agent in that same iteration. The updating equation (Equation (17)) calculates the new position for each agent by considering the position variables of the leaders and adjusting them based on the specified relationship. The parameter ρ is determined as a function of the current and maximum iteration numbers indicated by it and Max_{it}, while $\vec{r}_1$ and $\vec{r}_2$ are random vectors.

Following the update of the agents' positions, the leaders are refreshed with the top-performing agents in each iteration of the optimization process.

3.1.3. Stopping Criteria and Reporting the Best Leader

The DHL algorithm incorporates specific stopping criteria, namely the maximum number of iterations and convergence, to govern the termination of the main optimization loop. The algorithm stops its iteration after reaching a designated number of iterations. Additionally, the algorithm stops when the change in the objective function value for the best leader between consecutive iterations falls below a predefined tolerance level. This signifies that the optimization process has converged to a solution, eliminating the need for further iterations. By employing these stopping criteria, the DHL algorithm ensures control over computational resources while ensuring that an acceptable solution has been attained. At the end, the DHL algorithm provides the F^* and X^* for the problem.

3.2. Implementation and Framework

The flowchart of the framework for finding best charging strategy for EVs in the grid is shown in Figure 1.
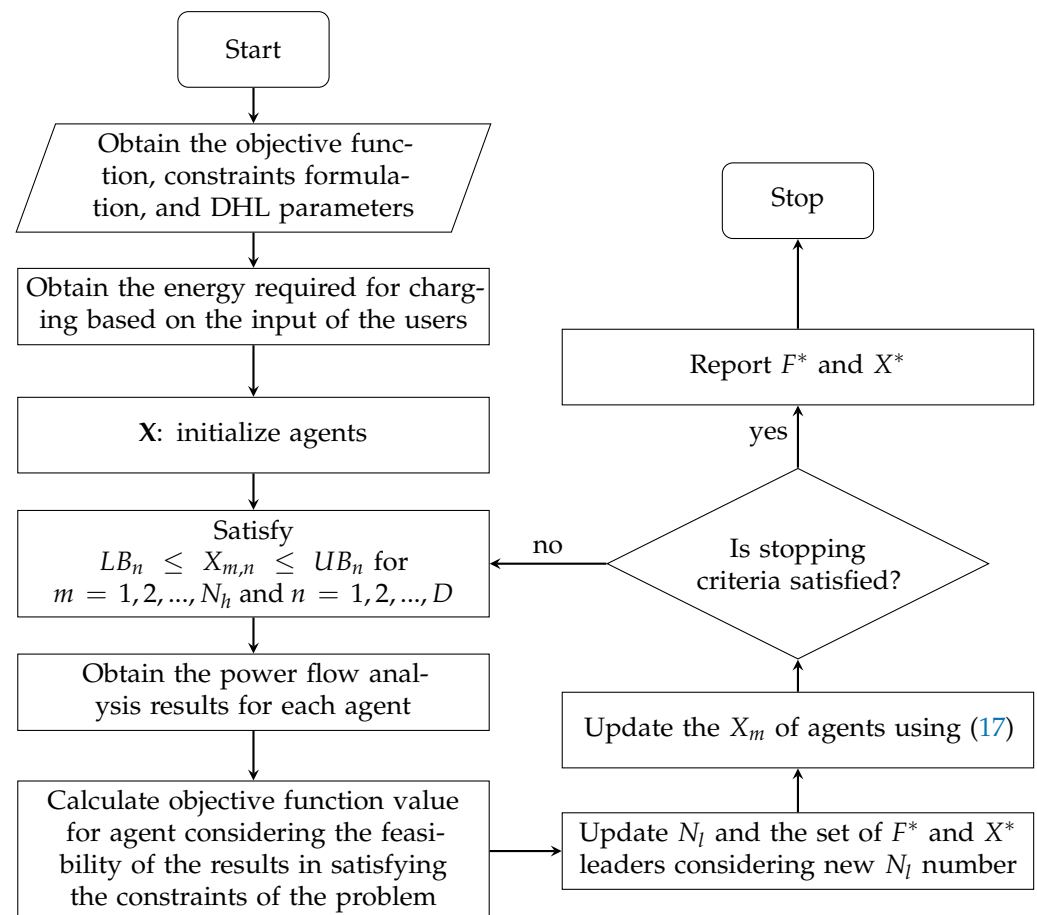

Figure 1. Flowchart of the EV charging optimization framework based on the DHL algorithm.

4. Test Systems and Scenarios

4.1. Test System

In this paper, the simulation study makes use of the IEEE 33 bus distribution systems described in [9]. The main improvements in these models revolve around integrating PV units and ESDs at different buses of the IEEE 33 bus system, called a local energy community in this research. The grid's arrangement is depicted in Figure 2.
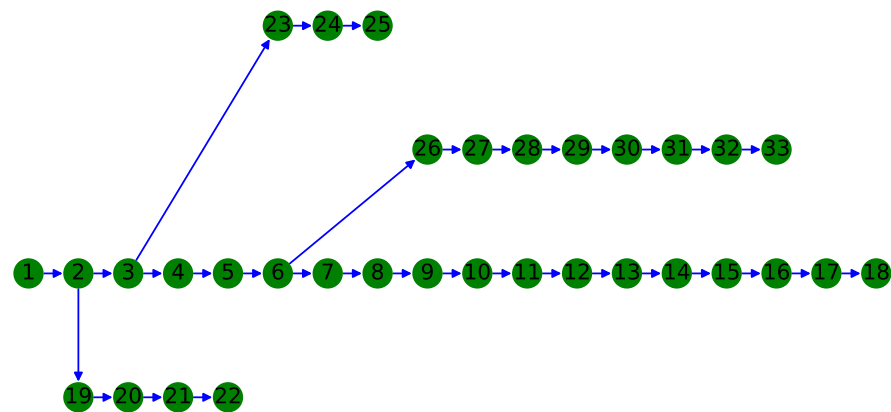
Figure 2. IEEE 33 bus system configuration.

Real data on load curve behavior and solar irradiation are utilized to create models for PV output and load characteristics. The test systems incorporate PVs, EVs (both residential and parking stations), and ESDs, and their locations and sizes in the IEEE 33 bus grid are provided in [44].

In the grid, the PVs, EVs, and ESDs are associated with an energy community in the grid. The energy communities in the low-voltage grid are connected to medium-voltage grids, except for the slack bus of the grid. The characteristics of these energy communities are modeled considering the real data provided by the Aardehuizen community in Olst, The Netherlands, as documented in [45].

The Aardehuizen community, as depicted in Figure 3, consists of 23 residential homes and a communal place, all dedicated to environmentally responsible living. The homes are constructed using sustainable materials, and the community strives to fulfill its energy needs through the use of sustainable sources such as PVs. Based on a multi-objective optimization for the PV and ESD units' sizing problem in [46], the size of the units in each community is modeled. To model the base load (including the demand, PV sizes, outputs, and ESS scheduling) of various energy communities connected to the IEEE 33 bus systems, multiple Pareto optimal solutions achieved with different parameters for sizing from [44] are employed. Additionally, the test cases in the subsequent sections consider different levels of EV penetration in each local community.
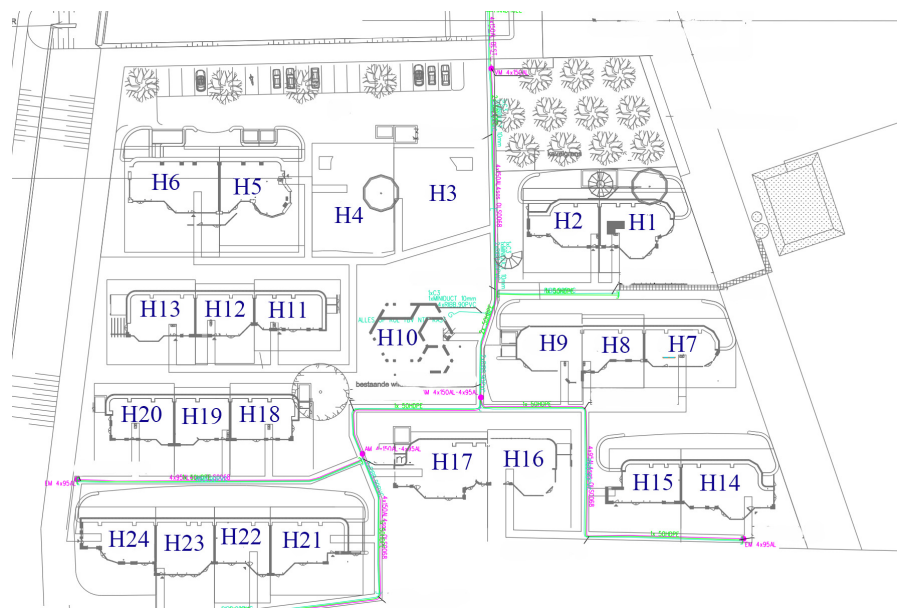

Figure 3. The Aardehuizen community configuration.

4.2. Test Scenarios for the Optimization Problem

To minimize the amount of data as input from the EV users, the formulation needs to estimate the amount of energy $E_{i,er}^{EV}$ based on kilometers added by the user. Using this method, the initial state of charge for the EVs and the capacity of the batteries in the equations can be replaced by $E_i^{ini} = 0$ and $\overline{E}_i^{EV} = E_{i,er}^{EV}$.

Different test scenarios are modeled by assuming different user inputs ($E_{i,er}^{EV}$) and also different numbers of EVs (both residential and public parking stations) connected to each node of the system. Note that the framework is designed to work as an online energy management system, and, by changing the input data in the real-time scheduling, it adopts the charging scheduling for EV charging. However, here, we assumed several offline scenarios based on the data provided in [44]. The k_1 and k_2 parameters in the objective function are determined as $1000 \times \sum_{j=1}^{N_{BUS}} (V_{i,j} - V_{i,j,ref})^2$ for the base case scenario in which no EV connected to the chargers.

The test case scenarios for validating the effectiveness of the framework are as follows:

- Charging scheduling of the public charging stations.
- Charging scheduling of the residential EVs.
- Charging scheduling of all EVs.

Note that several classes of EV numbers connected to the chargers are also tested for each scenario. Note that each node of the IEEE 33 system has a public parking place and can host a maximum of 10 EVs. The maximum number of EVs for the parking places is assumed as 320 EVs. Additionally, the assumption for residential EVs is one EV per household, so 736 EVs in total.

5. Results and Discussion

The main usage of the framework is to coordinate the charging strategy of any number of EVs in the grid for day-ahead optimization. Based on this assumption, the test cases are tested for different days of the year and also different numbers of EVs connected to the chargers. Note that for modeling the charging energy requirements (CERs) of the EV user, we used a set random number with an average travel duration of 30 km for the residential users and 50 km for the EVs in the parking station based on the data provided in [47]. Based on the assumptions for consumption of different EV models and user input, the CER is estimated for each car. Note that the data for the conversion are provided in [47,48]. The optimization of the EV charging scheduling is based on discrete time intervals for a representative day with a 15 min resolution.

The number of agents in the DHL algorithm and the maximum number of iterations are set to 30 and 500, respectively. Note that for test scenarios, the secondary stopping criteria are activated if the algorithm converges, but, for the performance comparison, only the fixed stopping criteria are assumed for the fare comparison. We used a PC with a 3.6 GHz i-7 processor and 16GB RAM to perform the tests using Python. For the power flow, the framework uses the Laurent power flow [49] to calculate the voltages of the nodes. The power flow method can handle the radial and mesh configuration of the grid, and it can utilize the effect of an unbalanced load in the formulations.

5.1. Test Scenarios

For each test scenario, the charging strategy of the near-optimal strategy (called Near-optimal) found by the framework is compared with the worst strategy and slow charging strategy. The worst scheduling (called Worst strategy) for charging EVs is defined as starting to charge the EVs at maximum charging power from the time at which the EVs are connected to the chargers. Additionally, the slow charging strategy (called Slow charging) is defined as slow charging all of the EVs with 6 Amp until the time at which the EVs are disconnected. Note that 6 Amp or the maximum charging power is used in Equation (10).

5.1.1. Charging Scheduling of the Public Charging Stations

For this scenario, the EVSC framework only manages the charging strategy of EVs in public charging stations. The framework is tested for a random day of the data provided in [44] and three scenarios of EV numbers. The scenarios are for 50%, 75%, and 100% of the EV charger slots occupied by EVs.

For the scenario with 50% parking EVs (P-EVs), the CER and the number of EVs per node in the system are shown in Figure 4. For this scenario, the total amount of energy required by EV users is 1.74 MWh. In the worst-case strategy, the ENS component of the objective function is zero. We are comparing this worst-case charging schedule with two other scenarios: a near-optimal schedule determined by the framework and a slow charging scenario. We are evaluating these scenarios based on the objective function's value, voltage violations, and ENS.
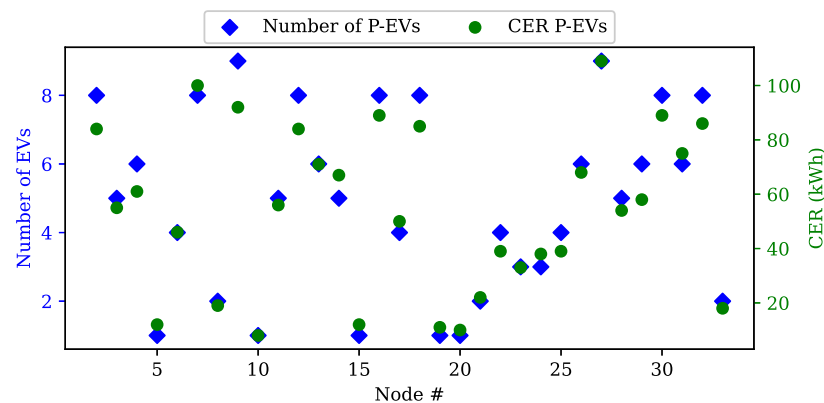
Figure 4. The number of EVs per local community and CER for 50% penetration of public parking EVs.

Based on the results of the scenarios in Table 1, with 50% P-EVs while supplying all the energy required by users, the system can operate without any voltage violations. The effect of aggregated powers on the base load profile of the system for different scenarios is shown in Figure 5. The results indicate that the framework aimed to maximize the utilization of power generated by PV units and shifted the required charging energy for users to off-peak periods during the simulation day.
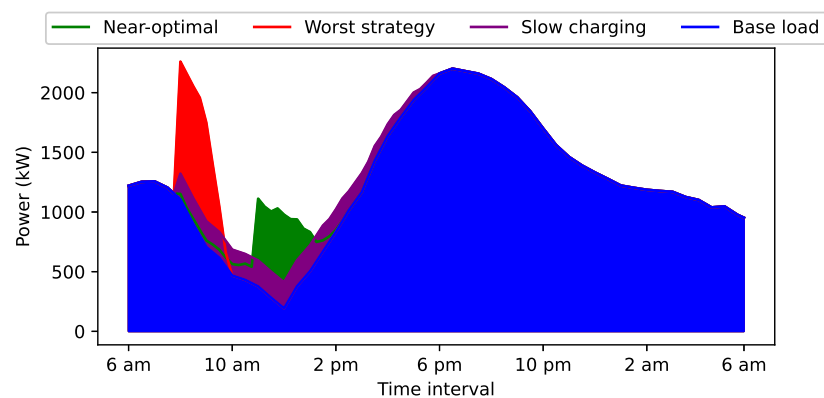

Figure 5. The effect of aggregated powers of 50% P-EVs on the base load profile of the system.

The amount of charging energy required for each node of the system for a scenario with 75% parking P-EVs is shown in Figure 6. The total amount of energy required by EV users in this scenario is 2.70 MWh. Based on the Worst, Slow, and Near-optimal solutions' results in Table 1, there is no voltage violation for the Slow and Near-optimal solutions. The objective function for the Worst strategy solution is 200.7984, which indicates that the solution has a regain of 200 for the violation in the simulation period. The effect of the

charging strategies on the minimum voltage magnitude values in the voltage profile of the system is shown in Figure 7.

Table 1. Detailed information for the different types of strategies for charging P-EVs.

P-EVs %	Type of Strategy	OF	PVV	ENS
50%	Worst strategy	0.7351	0	0
	Slow charging	0.6838	0	0
	Near-optimal	0.6707	0	0
75%	Worst strategy	200.7984	200	0
	Slow charging	0.7041	0	0
	Near-optimal	0.6953	0	0
100%	Worst strategy	3100.8933	3100	0
	Slow charging	0.7348	0	0
	Near-optimal	0.7304	0	0
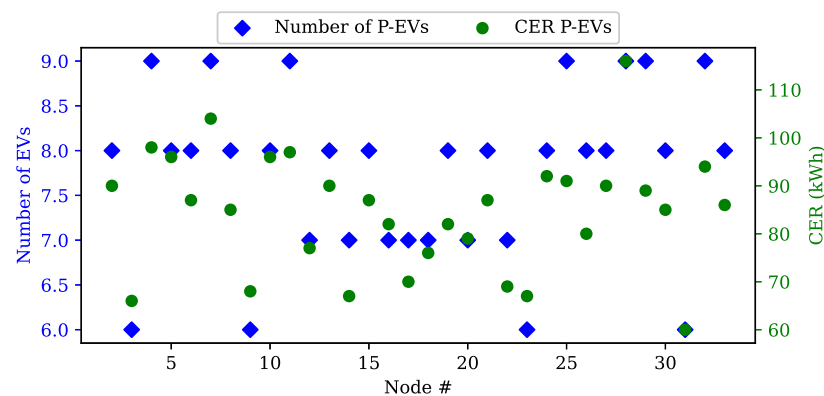
Figure 6. The number of EVs per local community and CER for 75% penetration of public parking EVs.
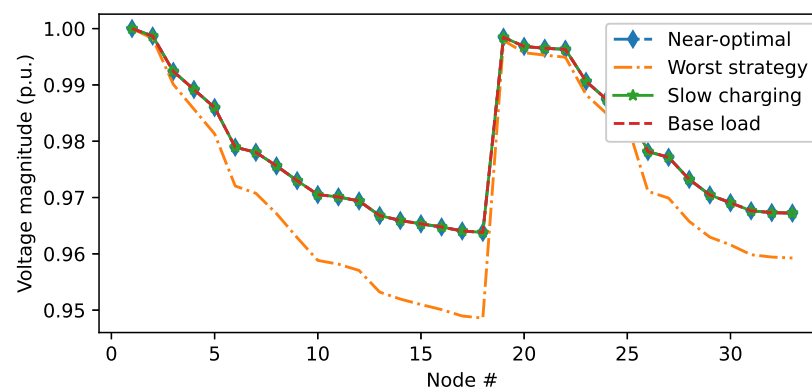

Figure 7. The effect of aggregated powers of 75% penetration of P-EVs on the minimum voltage magnitude of the nodes.

The impact of charging scheduling on the power profile of the system is illustrated in Figure 8. The worst charging strategy resulted in a new peak in power demand at 9 a.m., which caused congestion and under-voltages in almost all nodes of the system.

A scenario with 10 EVs is used for the last scenario of the number of P-EVs per node. For this scenario, the total CER for the P-EVs is 3.59 MWh, and the total CER per node for the EVs is shown in Figure 9. Increasing the number of P-EVs by 25% compared to the previous scenario has raised the objective function value for the Worst scheduling to 3100.8933. For this solution, the PVV is found as 3100, while the penalty functions for voltage violation in the Slow and Near-optimal solutions are found to be zero. Compared

to the previous scenario, the created power peak by P-EV charging in the Worst solution is even larger, as shown in Figure 10. The peak load is the reason for the voltage violations, as shown in Figure 11. Note that the minimum voltage magnitude for the grid is found to be 0.96 p.u for the Near-optimal and Slow charging solutions, while it is 0.93 p.u for the Worst scheduling solution. Figure 12 depicts the surcharging strategy for a random P-EV connected to a charger at node 33 of the test system. The figure showcases the charging strategies for the Worst, Slow, and Near-optimal solutions, allowing for comparison.
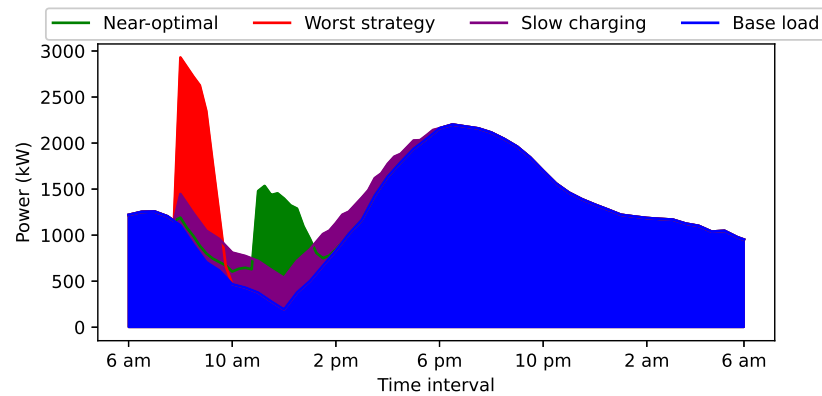

Figure 8. The effect of aggregated powers of 75% P-EVs on the base load profile of the system.
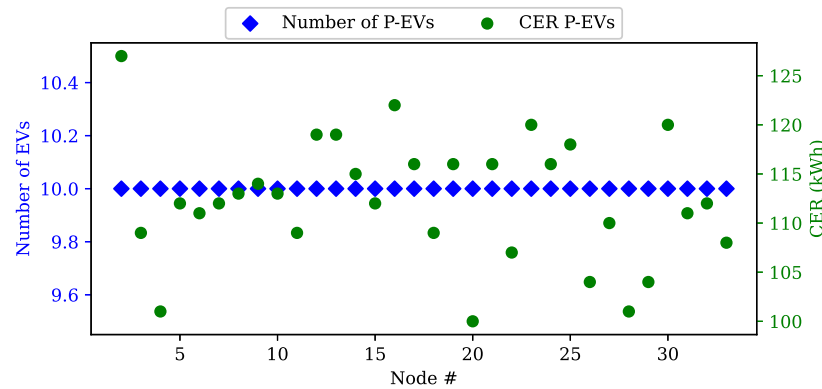

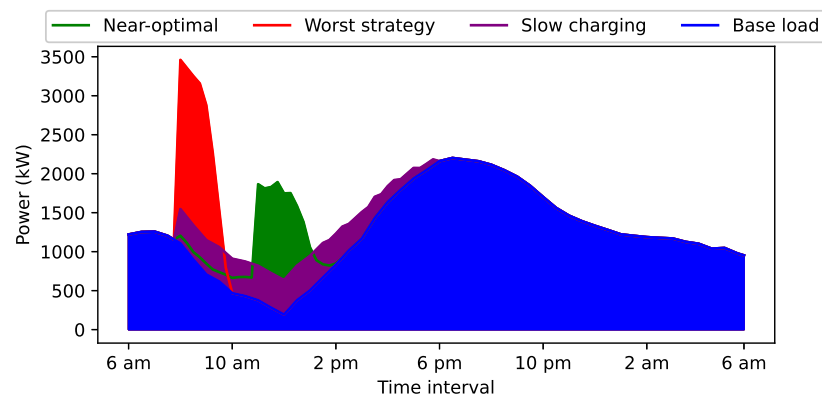**Figure 9.** The number of EVs per local community and CER for 100% penetration of public parking EVs.

Figure 10. The effect of aggregated powers of 100% P-EVs on the base load profile of the system.
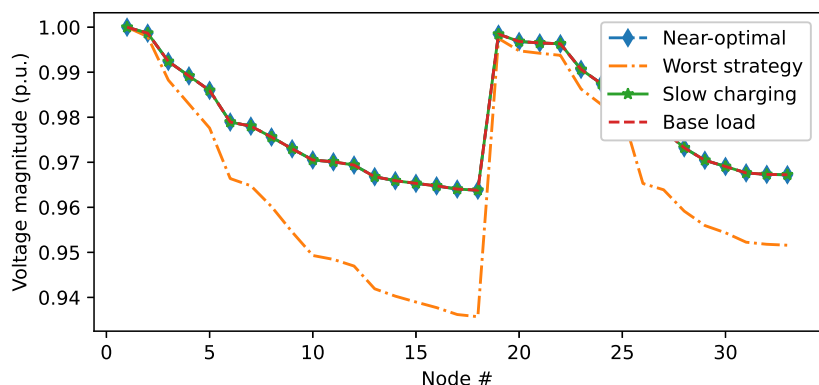
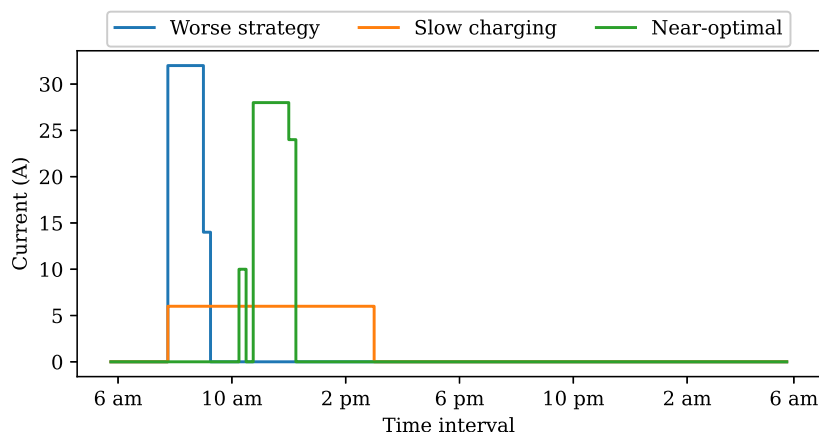**Figure 11.** The effect of aggregated powers of 100% penetration of P-EVs on the voltage profile of the system.

Figure 12. The charging schedules for a random EV at node 33 with 10 kWh CER.

5.1.2. Charging Scheduling of the Residential EVs

For this scenario, the optimization framework only manages the charging strategy of residential EVs (R-EVs). The framework is tested for the same day of the data and the same base load for the system as the previous scenario. Three penetration scenarios for R-EVs are for 50%, 75%, and 100% of households that want to charge EVs.

The results for the charging strategy solutions considering the objective function and penalty function values are shown in Table 2. Unlike the previous scenario for the P-EVs charging strategy, in this case, the Slow charging strategy will not prevent the violation in the system. Based on the results for all the penetration levels, only the Near-optimal strategy found by the framework can supply all of the R-EVs with the required energy while using smart scheduling to eliminate all the under-voltage problems. Note that the total CER for each node of the distribution system and the number of R-EVs connected to the residential chargers are shown in Figure 13a for 50%, Figure 13b for 75%, and Figure 13c for 100% penetration of R-EVs.

Table 2. Detailed information for the different types of strategies for charging R-EVs.

R-EVs %	Type of Strategy	OF	PVV	ENS
50%	Worst strategy	5800.9153	5800	0
	Slow charging	0.8101	0	0
	Near-optimal	0.7454	0	0
75%	Worst strategy	7601.1457	7600	0
	Slow charging	1200.9059	1200	0
	Near-optimal	0.8056	0	0

Table 2. *Cont.*

R-EVs %	Type of Strategy	OF	PVV	ENS
	Worst strategy	7901.4006	7900	0
100%	Slow charging	5900.9939	5900	0
	Near-optimal	0.8604	0	0

(**a**) 50% penetration.

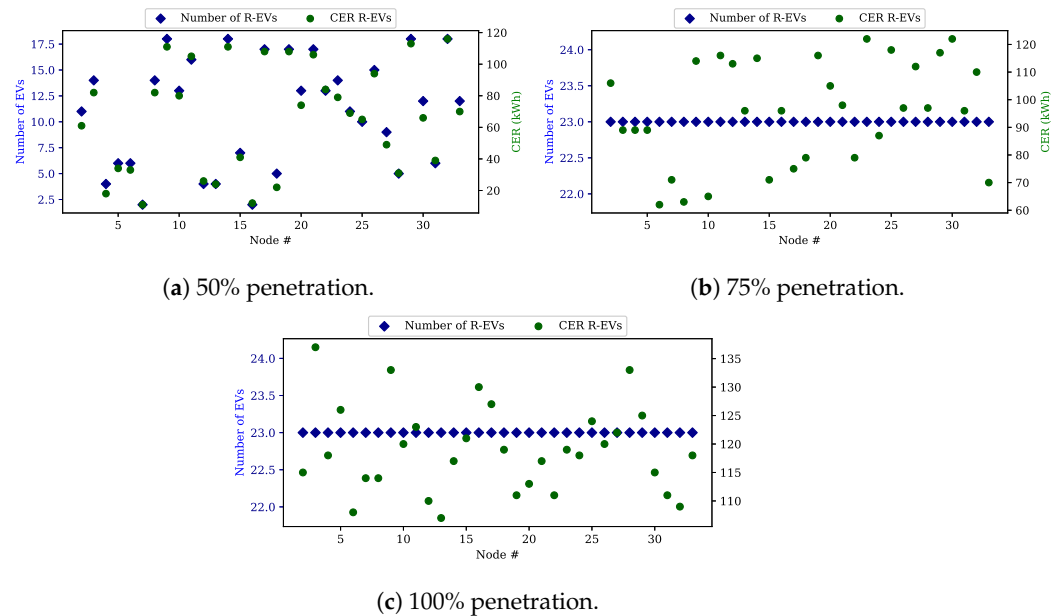(**b**) 75% penetration.

(**c**) 100% penetration.

Figure 13. The number of EVs per local community and CER for different penetration of R-EVs.

The voltage profiles of the system for all the strategies and penetration levels are shown in Figure 14. As shown in Figure 14a–c, compared to Figure 14d, the profiles are within the boundaries for the normal operation of the system. For the Near-optimal cases, the minimum voltage magnitude is calculated as 0.96 p.u. In the other cases, the charging strategy in the Slow and Worst solution created violations (shown with dark blue color in the figures). The minimum voltage magnitudes for the Slow charging solution are found to be 0.95 p.u for 50%, 0.94 p.u for 75%, and 100% R-EV penetration levels. For the Worst strategy, in which it charges the cars as soon as possible, the drop in voltage is so high that in the real test system, it will create a black-out in the system. The voltage magnitudes for different penetration levels of the R-EV are 0.91 p.u for 50% penetration, 0.87 p.u for 75% penetration, and 0.85 p.u for 100% penetration of the cars in the households.

The power profile on the chosen day for the base load of the system indicates a maximum power of 2.2 MW. However, when employing the Worst solution for charging the R-EVs, the peak power levels significantly increase to a range from 4.7 to 6.8 MW, depending on the penetration level of the R-EVs. On the other hand, the peak power for the Slow charging strategy solutions is observed to be within the range from 2.7 to 3.1 MW. These results underscore the significance of smart scheduling, as it successfully redistributes the charging power to non-peak times, preventing any escalation in peak power consumption. Figure 15 illustrates the power profiles for various levels of R-EV penetration.

The minimum voltage magnitudes are found for nodes 18 and 33 of the test system. The charging strategies for a random household in the mentioned nodes are shown in Figure 16a,b. Note that the charging strategies are shown for different solutions, and for both EVs, the CER is around 8 kWh.
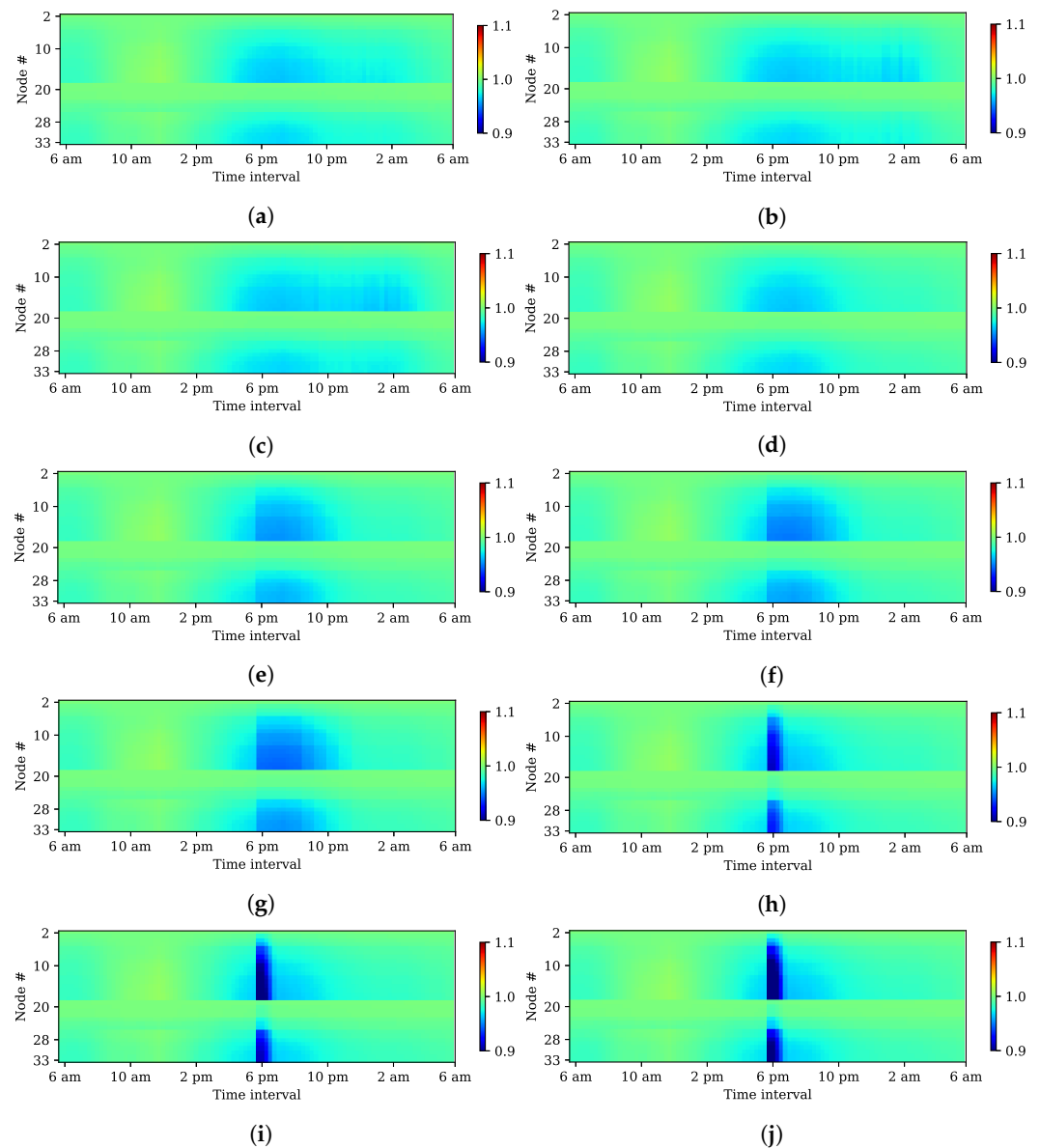
Figure 14. The effect of aggregated powers of different penetration of R-EVs on the voltage profile of the system. (**a**) Near-optimal P-EVs scheduling for 50% R-EV; (**b**) Near-optimal P-EVs scheduling for 75% R-EV; (**c**) Near-optimal P-EVs scheduling for 100% R-EV; (**d**) Voltage profile for the test system with no EV; (**e**) Slow charging for R-EVs for 50% R-EV; (**f**) Slow charging for R-EVs for 75% R-EV; (**g**) Slow charging for R-EVs for 100% R-EV; (**h**) Worst P-EV charging strategy for 50% R-EV; (**i**) Worst P-EV charging strategy for 75% R-EV; (**j**) Worst P-EV charging strategy for 100% R-EV.

5.1.3. Charging Scheduling of All EVs

In this section, we conduct tests on a realistic scenario in which a random number of EVs are connected to the chargers. The objective is to evaluate the impact of charging scheduling on the operation of the system for different days of the year.

By implementing smart charging strategies across various days of the year, we aim to demonstrate the effectiveness of these approaches in light of the diverse base power profiles of the system. This includes variations in the base load curve as well as distributed generation levels. Through these experiments, we can assess how well smart charging adapts to different system conditions and optimizes the overall operation.

Three random days, each representing a season of the year, are tested in this section. A day in February represents winter, a day for summer is based on the DG and load curve

of August, and, finally, a random day in November represents the behavior of fall/spring. Note that in previous sections, a random day in July was tested for smart charging.
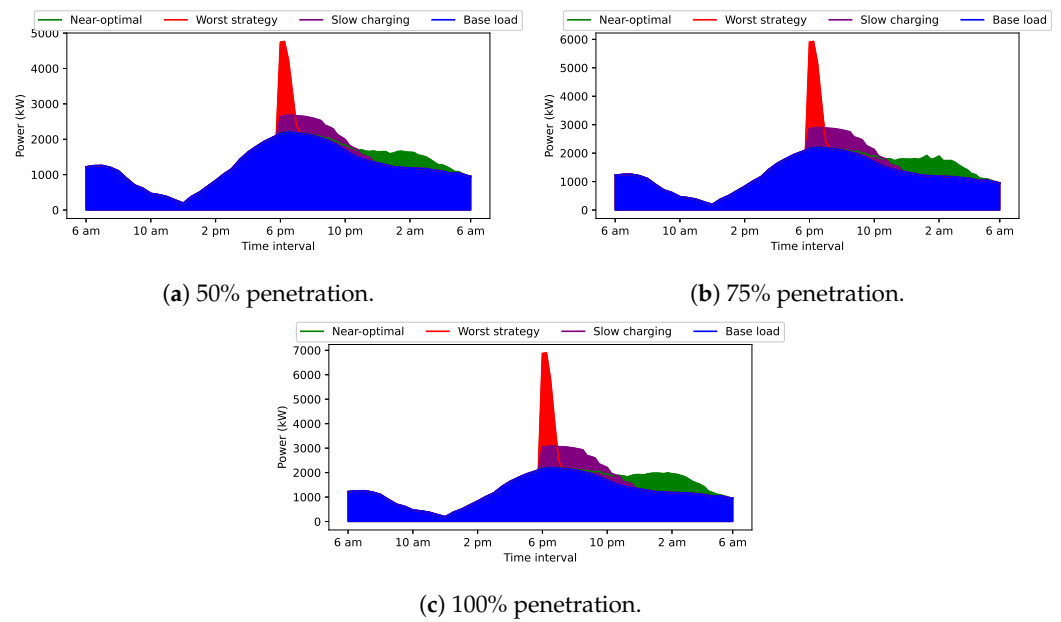

(**a**) 50% penetration.

(**b**) 75% penetration.

(**c**) 100% penetration.

Figure 15. The effect of aggregated powers of different penetration of R-EVs on power profile of the distribution system.
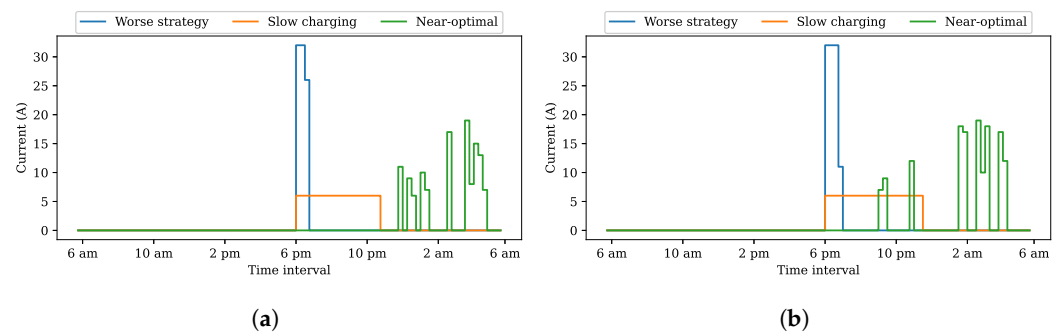

(**a**)

(**b**)

Figure 16. The charging strategy for a random R-EV with 100% penetration of EVs. (**a**) The charging strategy for a random EV in node 18 of the system. (**b**) The charging strategy for a random EV in node 33 of the system.

The total CER for the R-EVs is 2.2 MWh, and, for the P-EVs, it is 1.7 MWh for a February day. The total CER values for an August day are 2.6 MWh for the R-EVs and 2.1 MWh for the P-EVs, and, for a November day scenario, the values are 2.6 and 1.9 MWh for the R-EVs and P-EVs, respectively. The base load and the effect of the charging strategies on the power profiles are shown in Figure 17. Based on the results, the worst charging strategy will increase the peak power by 139%, 164%, and 147% for the February, August, and November day scenarios. By increasing the peak powers for different day scenarios using the Slow strategy for charging EVs, the results are 75% for the February scenario, 77% for August, and 72% for the November scenario. Note that the maximum percentage in increasing the peak load is 88% for the P-EVs using Near-optimal solutions.

The results suggested that the voltage profile of the system is without any voltage violation for smart charging, and it eliminated all the violations created by charging the EVs. The minimum voltage magnitudes for the February day are found to be 0.88, 0.95, and 0.95 p.u for the Worst, Slow, and Near-optimal solutions. For the August day, the minimum voltage magnitude for the Worst solution was found to be 0.89, and for the Slow and Near-optimal solutions, it was found to be 0.95 p.u. The same values are found for the

November scenario. The minimum voltage magnitudes per node for each day are shown in Figure 18.
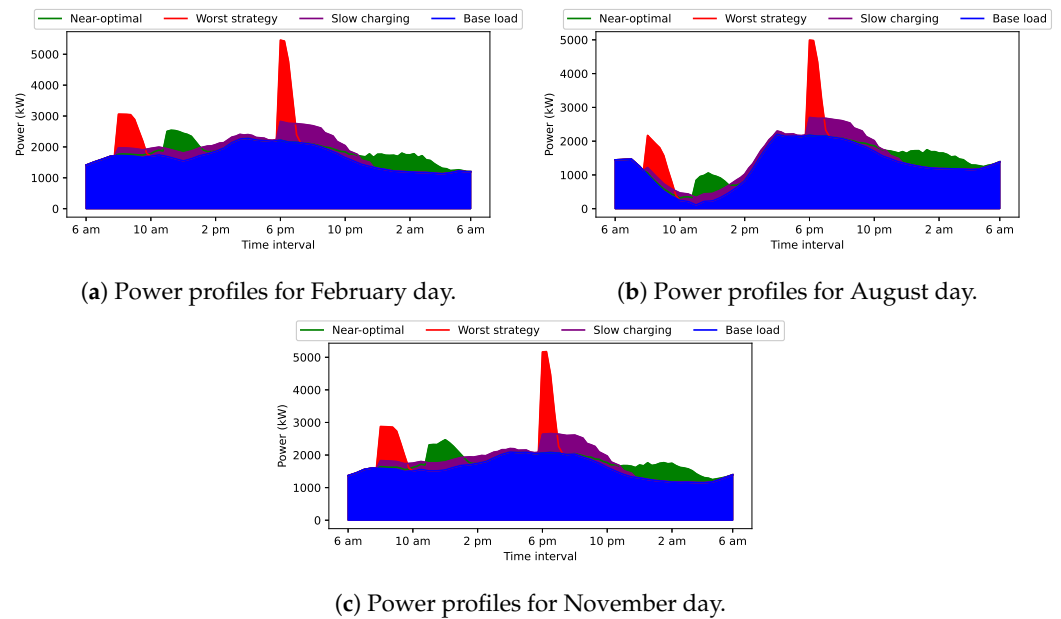

(**a**) Power profiles for February day.

(**b**) Power profiles for August day.

(**c**) Power profiles for November day.

Figure 17. The effect of aggregated powers of EVs on the power profile of the distribution system for different days of a year.

The number of public chargers occupied by EVs at node 33 of the system for a February day is seven, while 16 households required charging energy for their cars on the same day. The differences between the charging strategies for each car are shown in Figure 19. Note that the charging strategy of cars for other days located at node 25 (for an August day) and 22 (for a November day) is also shown in Figures 20 and 21.
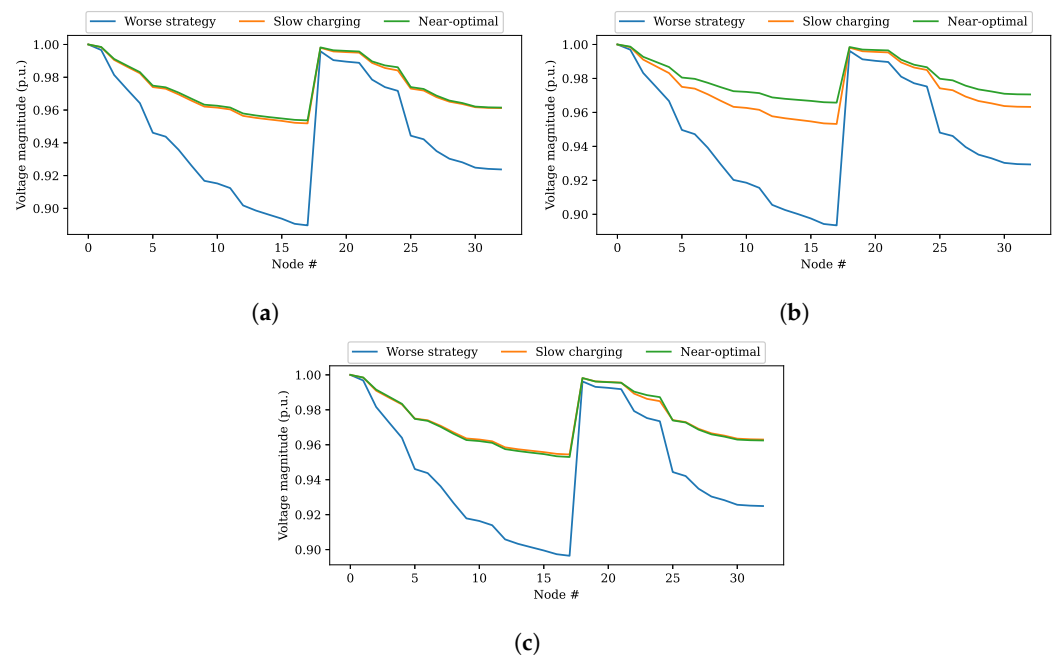

(**a**)

(**b**)

(**c**)

Figure 18. Minimum voltage magnitude per node of the distribution system for different days of a year. (**a**) Minimum voltage magnitude per node for February day. (**b**) Minimum voltage magnitude per node for August day. (**c**) Minimum voltage magnitude per node for November day.
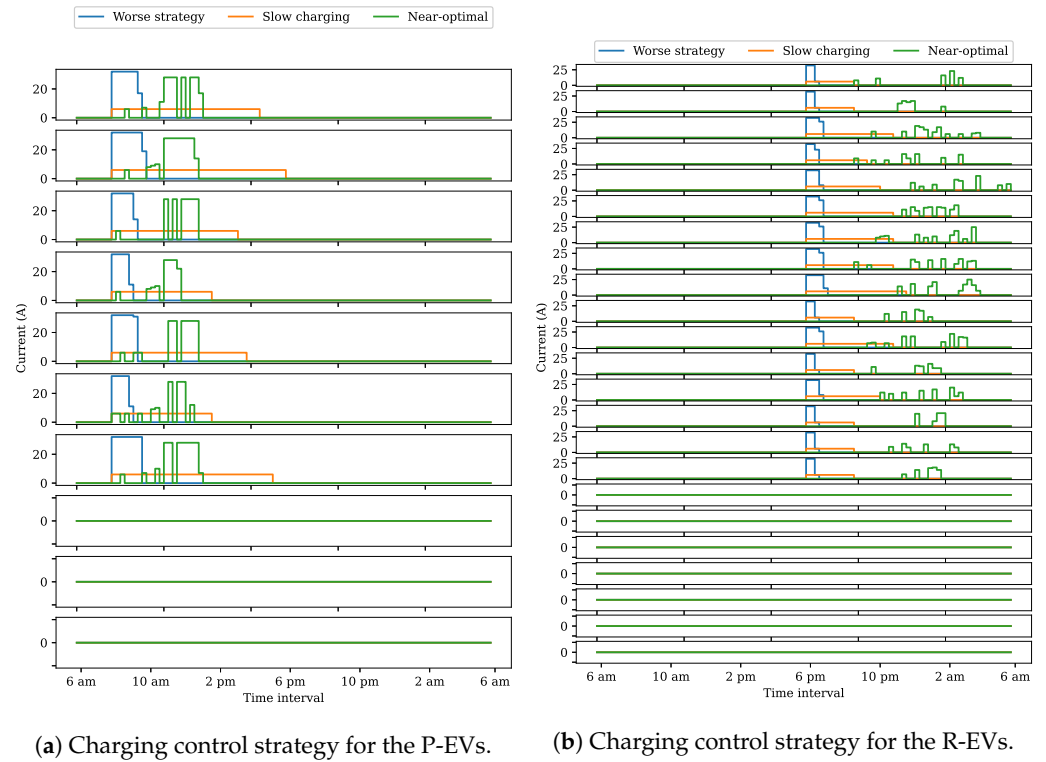
(**a**) Charging control strategy for the P-EVs.

(**b**) Charging control strategy for the R-EVs.

Figure 19. The charging control strategy for the EVs in February day scenario connected to the chargers in node 33 of the system.

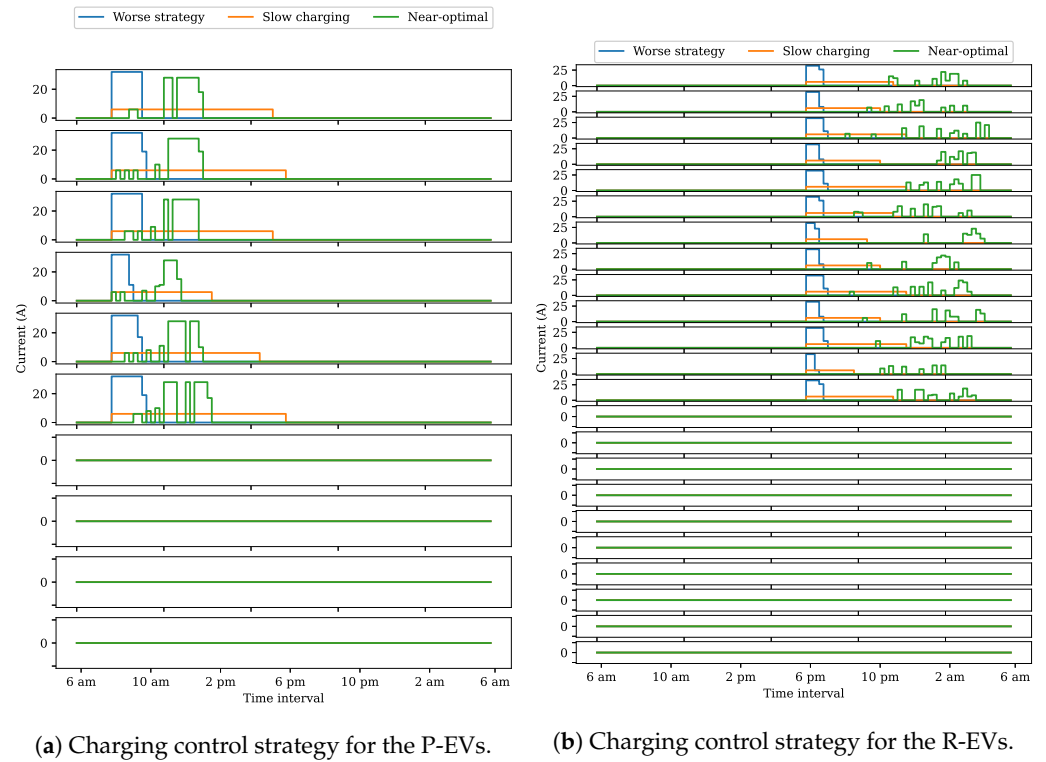(**a**) Charging control strategy for the P-EVs.

(**b**) Charging control strategy for the R-EVs.

Figure 20. The charging control strategy for the EVs in August day scenario connected to the chargers in node 25 of the system.

(**a**) Charging control strategy for the P-EVs.

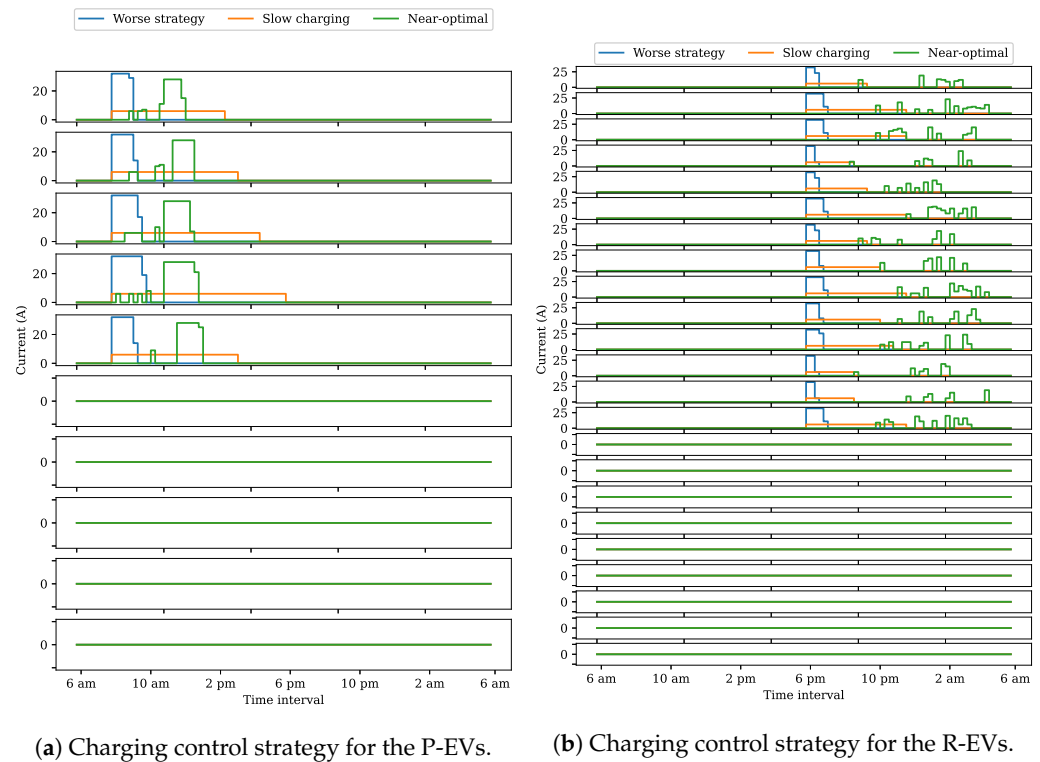(**b**) Charging control strategy for the R-EVs.

Figure 21. The charging control strategy for the EVs in November day scenario connected to the chargers in node 22 of the system.

5.2. Performance of Optimization Algorithm

In order to establish the superiority of the DHL algorithm, we conducted a comprehensive evaluation that involved comparing the solutions obtained for EV charging by the framework using DHL with those obtained using other heuristic algorithms. This comparative analysis was conducted to demonstrate the DHL algorithm's ability to identify near-optimal solutions, offering additional validation for the charging strategies presented in this paper.

Table 3 presents the objective function values obtained by the framework using the DHL algorithm in comparison to other heuristic algorithms, namely Grey Wolf Optimization (GWO) [50] and Particle Swarm Optimization (PSO) [10]. All methods were run for the same number of iterations without considering the second criterion for a dynamic stop.

Table 3. The detailed comparison of the performance of the DHL algorithm used in the framework with results found by GWO and PSO methods.

		DHL				GWO				PSO			
		Mean	Std.	Best	Worst	Mean	Std.	Best	Worst	Mean	Std.	Best	Worst
R-EVs	F value	0.9895	0.0001	**0.9893**	0.9896	0.9895	0.0001	0.9894	0.9896	0.9895	0.0001	0.9894	0.9896
	ET [s]	**96.9**	0.23	96.7	97.2	119.6	0.23	119.3	119.9	119.1	0.32	118.6	119.6
P-EVs	F value	1.0026	0.0001	**1.0024**	1.0027	1.0027	0.0001	1.0026	1.0029	1.0026	0.0001	1.0025	1.0027
	ET [s]	**94.3**	0.79	93.2	95.1	118.8	1.07	117.5	119.6	112.5	0.06	112.4	112.9
All EVs	F value	1.0783	0.0001	1.0782	1.0783	1.0784	0.0002	1.0782	1.0785	**1.0782**	0.0001	0.0782	1.0783
	ET [s]	**105.9**	0.21	105.8	106.1	121.2	0.59	120.4	122.9	123.9	0.6	123.3	124.2

The simulations were conducted for the test systems for a random day scenario with a random CER value for three cases of scheduling for the charging of R-EVs, P-EVs, and all EVs. The maximum number of iterations was set to 20. This implies that the optimization process was run for a total of 20 iterations to obtain the results. Note that 20 iterations is chosen based on the results of the framework using dynamic stopping criteria. Furthermore,

in the pursuit of employing heuristic methods, we established a fixed count of 30 solutions to be considered during the optimization process.

The PSO method offers a range of adjustable parameters that allow fine-tuning of the optimization process. In this study, we focused on the inertia weight, a crucial parameter that influences a particle's velocity and subsequent position. Initially, the inertia weight was set to 0.72. To enable a gradual reduction over the iterations, 0.9 is used as the damping ratio. The cognitive/social learning rates are also adjusted, for which each dictates how a personal best for a particle and its global best position affect its movement. Both parameters were set to 1.49 to update the positions.

It is worth noting that the values for these parameters were determined through careful experimentation, ensuring the PSO method's effectiveness. In contrast, the DHL and GWO methods are considered parameter-free, meaning they operate without requiring any extra parameter adjustments.

The table provides a comprehensive comparison of various methods concerning their performance measures. These measures encompass the average (mean), standard deviation (STD), and best objective function values derived from 50 independent runs. Additionally, the convergence speed of the heuristic methods is assessed by evaluating their computational time, represented as ET (execution time in seconds) in the table.

The results in Table 3 indicate that the best objective function values are found by the DHL method, and, for the mean values, the different methods are nearly identical across all scenarios. However, the DHL method stands out by providing the best solutions. This suggests that the DHL method yields more reliable solutions. Interestingly, the DHL method demonstrates a better performance in terms of mean computation times for all charging scenarios. This implies that the DHL method is more efficient in terms of computational speed compared to the other methods, providing faster solutions on average.

6. Conclusions

The electrification of transportation through the adoption of electric vehicles (EVs) presents a promising solution for achieving sustainable mobility and reducing greenhouse gas emissions. However, the ever-increasing deployment of EVs brings challenges for charging infrastructure and its impact on the electrical grid. To overcome these challenges, the smart charging approaches introduced in this paper can be used as solutions that optimize charging processes and contribute to the development of a smarter and more efficient grid.

This study has focused on the optimization of EVSC through a novel multi-objective optimization framework employing the DHL method. The framework considers technical and user-oriented objectives, such as minimizing voltage violations, ENS to EVs, and improving the voltage profile of the network. By incorporating realistic EV charger behaviors and addressing the problem as an MINLP problem, the framework offers an accurate representation of the charging process and enables efficient computational behavior.

The results obtained from the implementation of the proposed framework on a realistic network with heavy integration of EVs demonstrate the effectiveness of the DHL algorithm in minimizing conflicting objectives proposed based on technical and user-satisfaction aspects. The framework provides a road map for EV aggregators and EV owners, guiding them on how to charge EVs based on their preferences while minimizing adverse technical impacts on the grid. By optimizing the EVSC process, the framework contributes to the efficient integration of EVs into the existing grid infrastructure.

Based on the results, the framework can handle the charging scheduling of any number of EVs with a calculated CER based on the user inputs without affecting the normal operation of the grid. The framework results indicate that, for any day of the year, with or without DG-generated power, the smart charging of EVs can help the grid eliminate voltage violations and also avoid the blackouts caused by the heavy integration of EVs. Moreover, the solution provided by the framework ensures that the charging strategy of the

EVs will not increase the peak load. Finally, the framework ensures the ENS for the user is zero, meaning that the energy required is supplied by the charger using smart scheduling.

Overall, this study highlights the significance of smart charging approaches in enabling the effective and sustainable deployment of EVs. The effect of the optimization algorithm in finding near-optimal solutions for MINLP in the framework is optimized by using the DHL method. The results indicate that DHL can provide better quality solutions faster compared to the different methods used in the framework. Furthermore, for future research, more analysis is needed to determine the potential for new business models and revenue streams through value-added services and vehicle-to-grid (V2G) technology.

Author Contributions: Conceptualization, B.A.; Methodology, B.A.; Validation, B.A. and E.S.; Writing—original draft, B.A.; Writing—review & editing, E.S.; Supervision, E.S. All authors have read and agreed to the published version of the manuscript.

Data Availability Statement: Data will be available on request.

Conflicts of Interest: The authors declare that they have no known competing financial interests or personal relationships that could have appeared to influence the work reported in this paper.

References

1. Alhindawi, R.; Abu Nahleh, Y.; Kumar, A.; Shiwakoti, N. Projection of greenhouse gas emissions for the road transport sector based on multivariate regression and the double exponential smoothing model. *Sustainability* **2020**, *12*, 9152. [CrossRef]
2. Hussain, M.T.; Sulaiman, N.B.; Hussain, M.S.; Jabir, M. Optimal Management strategies to solve issues of grid having Electric Vehicles (EV): A review. *J. Energy Storage* **2021**, *33*, 102114. [CrossRef]
3. Reddy, M.S.K.; Selvajyothi, K. Optimal placement of electric vehicle charging station for unbalanced radial distribution systems. *Energy Sources Part A Recover. Util. Environ. Eff.* **2020**, 1–15. [CrossRef]
4. Fernandez, L.P.; San Román, T.G.; Cossent, R.; Domingo, C.M.; Frias, P. Assessment of the impact of plug-in electric vehicles on distribution networks. *IEEE Trans. Power Syst.* **2010**, *26*, 206–213. [CrossRef]
5. Haghnegahdar, L.; Chen, Y.; Wang, Y. Enhancing dynamic energy network management using a multiagent cloud-fog structure. *Renew. Sustain. Energy Rev.* **2022**, *162*, 112439. [CrossRef]
6. Yu, H.; Niu, S.; Shang, Y.; Shao, Z.; Jia, Y.; Jian, L. Electric vehicles integration and vehicle-to-grid operation in active distribution grids: A comprehensive review on power architectures, grid connection standards and typical applications. *Renew. Sustain. Energy Rev.* **2022**, *168*, 112812. [CrossRef]
7. Kaewdornhan, N.; Srithapon, C.; Liemthong, R.; Chatthaworn, R. Real-Time Multi-Home Energy Management with EV Charging Scheduling Using Multi-Agent Deep Reinforcement Learning Optimization. *Energies* **2023**, *16*, 2357. [CrossRef]
8. Deb, N.; Singh, R.; Brooks, R.R.; Bai, K. A review of extremely fast charging stations for electric vehicles. *Energies* **2021**, *14*, 7566. [CrossRef]
9. Ahmadi, B.; Arias, N.B.; Hoogsteen, G.; Hurink, J.L. Multi-Objective Advanced Grey Wolf Optimization Framework for Smart Charging Scheduling of EVs in Distribution Grids. In Proceedings of the 2022 57th International Universities Power Engineering Conference (UPEC), Istanbul, Turkey, 30 August–2 September 2022; pp. 1–6.
10. Ahmadi, B.; Younesi, S.; Ceylan, O.; Ozdemir, A. The Arithmetic Optimization Algorithm for Optimal Energy Resource Planning. In Proceedings of the 2021 56th International Universities Power Engineering Conference (UPEC), Middlesbrough, UK, 31 August–3 September 2021; pp. 1–6.
11. Gupta, S.; Maulik, A.; Das, D.; Singh, A. Coordinated stochastic optimal energy management of grid-connected microgrids considering demand response, plug-in hybrid electric vehicles, and smart transformers. *Renew. Sustain. Energy Rev.* **2022**, *155*, 111861. [CrossRef]
12. Yang, W.; Guo, J.; Vartosh, A. Optimal economic-emission planning of multi-energy systems integrated electric vehicles with modified group search optimization. *Appl. Energy* **2022**, *311*, 118634. [CrossRef]
13. Koengkan, M.; Fuinhas, J.A.; Teixeira, M.; Kazemzadeh, E.; Auza, A.; Dehdar, F.; Osmani, F. The capacity of battery-electric and plug-in hybrid electric vehicles to mitigate CO2 emissions: Macroeconomic evidence from European Union Countries. *World Electr. Veh. J.* **2022**, *13*, 58. [CrossRef]
14. Dik, A.; Omer, S.; Boukhanouf, R. Electric Vehicles: V2G for Rapid, Safe, and Green EV Penetration. *Energies* **2022**, *15*, 803. [CrossRef]
15. Mal, S.; Chattopadhyay, A.; Yang, A.; Gadh, R. Electric vehicle smart charging and vehicle-to-grid operation. *Int. J. Parallel Emergent Distrib. Syst.* **2013**, *28*, 249–265. [CrossRef]
16. Yilmaz, M.; Krein, P.T. Review of Benefits and Challenges of Vehicle-to-Grid Technology. In Proceedings of the 2012 IEEE Energy Conversion Congress and Exposition (ECCE), Raleigh, NC, USA, 15–20 September 2012; pp. 3082–3089.

17. Clairand, J.M.; Rodríguez-García, J.; Alvarez-Bel, C. Smart charging for electric vehicle aggregators considering users' preferences. *IEEE Access* **2018**, *6*, 54624–54635. [CrossRef]

18. Vickers, N.J. Animal communication: When i'm calling you, will you answer too? *Curr. Biol.* **2017**, *27*, R713–R715. [CrossRef] [PubMed]

19. Fang, X.; Li, J.; Yuan, Y.; Yuan, X. Decentralized Control Strategy for Participation of Electric Vehicles in Distribution Voltage Control. *Processes* **2023**, *11*, 2552. [CrossRef]

20. Mazhar, T.; Asif, R.N.; Malik, M.A.; Nadeem, M.A.; Haq, I.; Iqbal, M.; Kamran, M.; Ashraf, S. Electric Vehicle Charging System in the Smart Grid Using Different Machine Learning Methods. *Sustainability* **2023**, *15*, 2603. [CrossRef]

21. Al-Ogaili, A.S.; Hashim, T.J.T.; Rahmat, N.A.; Ramasamy, A.K.; Marsadek, M.B.; Faisal, M.; Hannan, M.A. Review on scheduling, clustering, and forecasting strategies for controlling electric vehicle charging: Challenges and recommendations. *IEEE Access* **2019**, *7*, 128353–128371. [CrossRef]

22. Tostado-Véliz, M.; Kamel, S.; Hasanien, H.M.; Arévalo, P.; Turky, R.A.; Jurado, F. A stochastic-interval model for optimal scheduling of PV-assisted multi-mode charging stations. *Energy* **2022**, *253*, 124219. [CrossRef]

23. Solanke, T.U.; Ramachandaramurthy, V.K.; Yong, J.Y.; Pasupuleti, J.; Kasinathan, P.; Rajagopalan, A. A review of strategic charging–discharging control of grid-connected electric vehicles. *J. Energy Storage* **2020**, *28*, 101193. [CrossRef]

24. Knez, M.; Zevnik, G.K.; Obrecht, M. A review of available chargers for electric vehicles: United States of America, European Union, and Asia. *Renew. Sustain. Energy Rev.* **2019**, *109*, 284–293. [CrossRef]

25. Chandwani, A.; Dey, S.; Mallik, A. Cybersecurity of onboard charging systems for electric vehicles—Review, challenges and countermeasures. *IEEE Access* **2020**, *8*, 226982–226998. [CrossRef]

26. Bitencourt, L.d.A.; Borba, B.S.; Maciel, R.S.; Fortes, M.Z.; Ferreira, V.H. Optimal EV Charging and Discharging Control Considering Dynamic Pricing. In Proceedings of the 2017 IEEE Manchester PowerTech, 2017, Manchester, UK, 18–22 June 2017; pp. 1–6.

27. Zargar, B.; Wang, T.; Pitz, M.; Bachmann, R.; Maschmann, M.; Bintoudi, A.; Zyglakis, L.; Ponci, F.; Monti, A.; Ioannidis, D. Power quality improvement in distribution grids via real-time smart exploitation of electric vehicles. *Energies* **2021**, *14*, 3533. [CrossRef]

28. Hadley, S.W.; Tsvetkova, A.A. Potential impacts of plug-in hybrid electric vehicles on regional power generation. *Electr. J.* **2009**, *22*, 56–68. [CrossRef]

29. Shariff, S.M.; Alam, M.S.; Hameed, S.; Khalid, M.R.; Ahmad, A.; Al-Ammar, E.A.; Alsaidan, I.; Alrajhi, H. A state-of-the-art review on the impact of fast EV charging on the utility sector. *Energy Storage* **2022**, *4*, e300. [CrossRef]

30. Vita, V.; Fotis, G.; Chobanov, V.; Pavlatos, C.; Mladenov, V. Predictive Maintenance for Distribution System Operators in Increasing Transformers' Reliability. *Electronics* **2023**, *12*, 1356. [CrossRef]

31. Staats, P.; Grady, W.; Arapostathis, A.; Thallam, R. A statistical analysis of the effect of electric vehicle battery charging on distribution system harmonic voltages. *IEEE Trans. Power Deliv.* **1998**, *13*, 640–646. [CrossRef]

32. Shi, Y.; Wang, H.; Shi, S. Relationship between social civilization forms and carbon emission intensity: A study of the Shanghai metropolitan area. *J. Clean. Prod.* **2019**, *228*, 1552–1563. [CrossRef]

33. Su, J.; Lie, T.; Zamora, R. A rolling horizon scheduling of aggregated electric vehicles charging under the electricity exchange market. *Appl. Energy* **2020**, *275*, 115406. [CrossRef]

34. Xiang, Y.; Hu, S.; Liu, Y.; Zhang, X.; Liu, J. Electric vehicles in smart grid: A survey on charging load modelling. *IET Smart Grid* **2019**, *2*, 25–33. [CrossRef]

35. Deng, Q.; Feng, C.; Wen, F.; Tseng, C.L.; Wang, L.; Zou, B.; Zhang, X. Evaluation of accommodation capability for electric vehicles of a distribution system considering coordinated charging strategies. *Energies* **2019**, *12*, 3056. [CrossRef]

36. Franco, J.F.; Rider, M.J.; Romero, R. A mixed-integer linear programming model for the electric vehicle charging coordination problem in unbalanced electrical distribution systems. *IEEE Trans. Smart Grid* **2015**, *6*, 2200–2210. [CrossRef]

37. Taghizadeh, S.; Hossain, M.; Lu, J.; Water, W. A unified multi-functional on-board EV charger for power-quality control in household networks. *Appl. Energy* **2018**, *215*, 186–201. [CrossRef]

38. Mediwaththe, C.P.; Smith, D.B. Game-theoretic electric vehicle charging management resilient to non-ideal user behavior. *IEEE Trans. Intell. Transp. Syst.* **2018**, *19*, 3486–3495. [CrossRef]

39. Deilami, S.; Muyeen, S. An insight into practical solutions for electric vehicle charging in smart grid. *Energies* **2020**, *13*, 1545. [CrossRef]

40. Yang, J.; He, L.; Fu, S. An improved PSO-based charging strategy of electric vehicles in electrical distribution grid. *Appl. Energy* **2014**, *128*, 82–92. [CrossRef]

41. Che, S.; Chen, Y.; Wang, L. Electric Vehicle Charging Station Layout for Tourist Attractions Based on Improved Two-Population Genetic PSO. *Energies* **2023**, *16*, 983. [CrossRef]

42. Giraldo, J.S.; Arias, N.B.; Vergara, P.P.; Vlasiou, M.; Hoogsteen, G.; Hurink, J.L. Estimating Risk-Aware Flexibility Areas for Electric Vehicle Charging Pools via AC Stochastic Optimal Power Flow. *J. Mod. Power Syst. Clean Energy* **2022**, *11*, 1247–1256. [CrossRef]

43. Ahmadi, B.; Giraldo, J.S.; Hoogsteen, G. Dynamic Hunting Leadership optimization: Algorithm and applications. *J. Comput. Sci.* **2023**, *69*, 102010. [CrossRef]

44. Ahmadi, B. IEEE 13, 33, and 123 Bus Distribution Systems Data, 2023. MATLAB Central File Exchange. Available online: https://www.mathworks.com/matlabcentral/fileexchange/123007-ieee-13-33-and-123-bus-distribution-systems-data (accessed on 9 January 2023).
45. Aardehuizen Community. Vereniging Aardehuis. Available online: https://www.aardehuis.nl/index.php/en/the-story/construction-phase (accessed on 10 April 2022).
46. Ahmadi, B.; Pappu, A.; Hoogsteen, G.; Hurink, J.L. Multi-Objective Optimization Framework for Integration of Distributed Energy Resources in Smart Communities. In Proceedings of the 2022 57th International Universities Power Engineering Conference (UPEC), Istanbul, Turkey, 30 August–2 September 2022; pp. 1–6.
47. Nijenhuis, B.; Doumen, S.C.; Hönen, J.; Hoogsteen, G. Using Mobility Data and Agent-Based Models to Generate Future E-Mobility Charging Demand Patterns. In Proceedings of the CIRED Porto Workshop 2022: E-mobility and power distribution systems, Porto, Portugal, 2–3 June 2022; Volume 2022, pp. 214–218. [CrossRef]
48. Ahmadi, B.; Ceylan, O.; Ozdemir, A. An Optimization Framework for Distributed Energy Resource Planning and Energy Management Strategy of Storage Devices and Electric Vehicles. In Proceedings of the 2022 2nd International Conference on Energy Transition in the Mediterranean Area (SyNERGY MED), Thessaloniki, Greece, 17–19 October 2022; pp. 1–6.
49. Giraldo, J.S.; Montoya, O.D.; Vergara, P.P.; Milano, F. A fixed-point current injection power flow for electric distribution systems using Laurent series. *Electr. Power Syst. Res.* **2022**, *211*, 108326. [CrossRef]
50. Mirjalili, S.; Mirjalili, S.M.; Lewis, A. Grey wolf optimizer. *Adv. Eng. Softw.* **2014**, *69*, 46–61. [CrossRef]